Low-temperature magnetic phase transitions of the geometrically frustrated isosceles triangular Ising antiferromagnet $CoNb_2O_6$

S. Kobayashi* and S. Mitsuda
Department of Physics, Faculty of Science, Science University of Tokyo, 1-3 Kagurazaka, Shinjuku-ku, Tokyo 162-8601, Japan

K. Prokes
Hahn-Meitner-Institute, SF-2, Glienicker Straße 100, D-14109 Berlin, Germany
(Received 25 July 2000; published 19 December 2000)

Low-temperature magnetic phase transitions of the geometrically frustrated isosceles triangular Ising antiferromagnet $CoNb_2O_6$ have been investigated by means of neutron diffraction down to $T=0.2$ K under applied fields up to $H_{\|c}=4.4$ kOe. Below $T\sim 0.6$ K, the relaxation time of the system becomes extremely long compared with our observation time, being responsible for all the anomalous low-temperature magnetic properties observed in the bulk measurements [T. Hanawa *et al.*, J. Phys. Soc. Jpn. **63**, 2706 (1994)]. In addition to confirmation of the triple point where the antiferromagnetic, field-induced ferrimagnetic, and incommensurate phases meet together in the $H_{\|c}-T$ magnetic phase diagram, we also found various ordered phases that are field induced between the ferrimagnetic and saturated paramagnetic phases.

DOI: 10.1103/PhysRevB.63.024415 PACS number(s): 75.30.Kz, 75.25.+z

I. INTRODUCTION

The triangular antiferromagnet with a partially released geometrical frustration has been attracting particular attention because of a possibility of the appearance of an unusual magnetic order absent in both frustrated and unfrustrated magnets.[1] As one of the model materials of such a system, we have studied in recent years a quasi-one-dimensional (quasi-1D) Ising magnet $CoNb_2O_6$, where the ferromagnetic zigzag chains along the *c* axis form an antiferromagnetic isosceles-triangular lattice in the *a-b* plane as shown in Figs. 1(a) and (b).[2–4] Neutron scattering has revealed that an isosceles-triangular geometry of frustrated spins produces interesting magnetic properties not found to date in any other magnetic materials, such as propagation-vector-dependent magnetic correlations[3] and anisotropic domain-growth kinetics.[4]

The magnetic phase diagram of $CoNb_2O_6$ under applied fields along the *c* axis has been extensively investigated by measurements of the bulk properties down to $T=0.5$ K by Hanawa *et al.*[5] as well as neutron-diffraction measurements down to $T\sim 1.5$ K by the authors[2,3] and Heid *et al.*[6] Neutron diffraction[2,3,6] showed that the system exhibits three magnetically ordered phases at low fields [sinusoidally amplitude-modulated incommensurate (IC) phase below $T_1\sim 3.0$ K, antiferromagnetic (AF) phase below $T_2\sim 1.9$ K, and field-induced ferrimagnetic (FR) phase], while at higher fields another ferrimagnetic state was observed around the phase transition from the FR to saturated paramagnetic (PM) phases.[6] All the ordered states are characterized by a propagation vector $\mathbf{Q}_{\text{propa}}=(0\ q\ 0)$, and the spins direct towards the two different easy axes shown in Fig. 1(a) reflecting the strong Ising character of the magnetic Co^{2+} spin. In previous measurements down to $T=1.5$ K,[3] we found that with decreasing temperature at lower fields, the IC region defined by both AF-IC and IC-FR first-order phase boundaries becomes narrower and the triple point where the AF, IC, and FR phases meet together might exist at a lower temperature. Our mean-field calculations for the isosceles-triangular-lattice Ising model with intrachain ferromagnetic interaction J_0 and interchain antiferromagnetic interactions J_1, J_2 (Ref. 3) not only qualitatively reproduced the $H_{\|c}-T$ magnetic phase diagram of $CoNb_2O_6$ in low-field region, but also successfully explained the anomalous broadening of the IC peak approaching the triple point.

In spite of the qualitative agreements between our mean-field results and neutron-diffraction results down to $T=1.5$ K, however, the low-temperature magnetic properties of this geometrically frustrated system were still not well understood. At $T=0.5$ K under applied fields along the *c* axis, an anomalous hysteresis in the magnetization process as well as a slow relaxation of the remanent magnetization have been found.[5] Particularly, the intermediate state with either one-third or two-thirds magnetization of the FR state was frequently field induced and persisted up to a highest measured external field of 2 kOe, while at higher temperatures

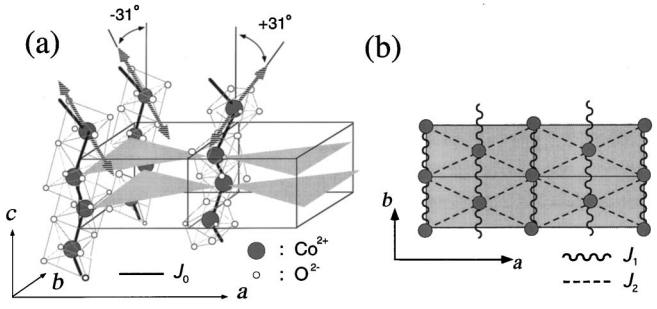

FIG. 1. (a) Chemical unit cell of $CoNb_2O_6$, where the zigzag chains are running along the *c* axis with the intrachain ferromagnetic coupling J_0. The hatched arrows represent the two different easy axes in the nearly *a-c* plane with a canting angle of $\pm 31°$, originated from the two different octahedral CoO_6 sites. (b) Isosceles triangular lattice with interchain antiferromagnetic interactions J_1 and J_2 in the *a-b* plane.

the FR state was always field induced. This indicates the presence of another stable magnetic phase at lower temperatures, or the appearance of a metastable state as was found in the antiferromagnetic-ferrimagnetic phase transition in the quasi-1D Ising system $FeCl_2 \cdot 2H_2O$.[7] Furthermore, the specific-heat measurements in zero field[5] revealed an additional low-temperature anomaly at $T_s \sim 0.65$ K below T_2, where a phase transition from the quasi-long-range AF ordering towards the true 3D long-range one below T_s was presumed.[3]

In this paper, we report low-temperature neutron-diffraction measurements down to $T=0.2$ K under applied fields up to $H_{\|c}=4.4$ kOe, where interesting low-temperature magnetic phase transitions inferred from the bulk measurements have been investigated.

II. EXPERIMENT

The single-crystal neutron-diffraction experiments on $CoNb_2O_6$ were carried out, using the two-axis diffractometer (E4), installed at Berlin Neutron Scattering Center (BENSC), in Hahn-Meitner Institute. A pyrolytic-graphite filter was used to eliminate second-order contamination. The collimation with 40′-40′-40′ from reactor to detector and incident neutrons with the wave length of 2.44 Å were used. In present experiments, the single crystal with dimensions $5 \times 5 \times 10\ mm^3$, grown by flux-growth technique[8] (sample B_{Co} in Ref. 3) was used. A vertical external field along the c axis up to 4.4 kOe as well as low temperatures down to 0.2 K were provided by the cryomagnet (VM-3) with a dilution refrigerator insert. Typical field-sweep rate was 6.7 (Oe/sec). All the scans taken on increasing external field were performed after zero-field cooling (ZFC) from the disordered PM state above $T_1 \sim 3.0$ K with a cooling rate of ~0.05 K/sec, while those taken on decreasing external field were carried out after putting the sample under the external field of $H_{\|c}=4.4$ kOe in the saturated PM state.

III. RESULTS AND DISCUSSION

A. Low-field region

In Figs. 2(a)–(d), we show the (3 k 0) reciprocal-lattice scans measured in increasing external field at several temperatures below T_2 after ZFC. From these scans, as shown in Fig. 3, the $H_{\|c}-T$ magnetic phase diagram was determined. As shown in Figs. 2 and 3, the AF ordering with $q=\frac{1}{2}$ was found to be stable in zero field down to the lowest temperature of $T=0.2$ K after ZFC. With increasing external field at $T=1.62$ K just below T_2, the field-induced first-order AF-IC phase transition occurs at $H_c^{\text{AF-IC}} \sim 225$ Oe and the broad IC peak with field-dependent q between $\frac{1}{3}$ and $\frac{1}{2}$ appears as shown in Fig. 2(a). With further increasing external field, the sharp FR peak at $k=\frac{1}{3}$ develops and the system enters the FR state at $H_c^{\text{IC-FR}} \sim 395$ Oe. When the external field decreases, the system exhibits the FR-IC and IC-AF phase transitions at lower fields as is documented by the data at $T=1.5$ K displayed in Fig. 3. Such two field-induced phase transitions were also observed at $T=1.0$ K, with pronounced hysteresis as shown in Figs. 2(b) and 3.

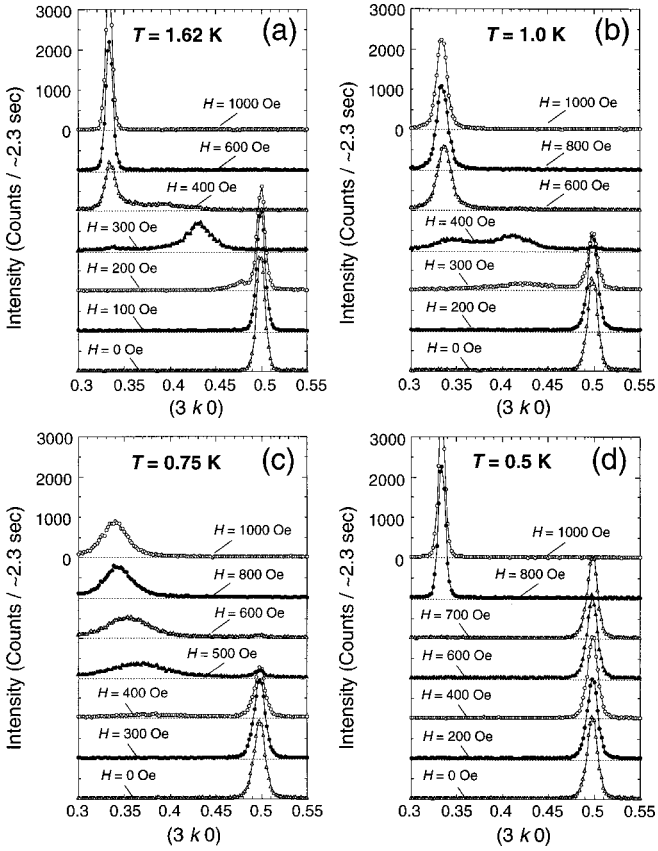

FIG. 2. Magnetic-field dependence of the (3 k 0) reciprocal-lattice scans in low-field region at several temperatures below T_2, (a) $T=1.62$ K, (b) $T=1.0$ K, (c) $T=0.75$ K, and (d) $T=0.5$ K.

At lower temperature of $T=0.75$ K, the field-induced AF-IC phase transition occurs at rather higher critical field of $H_c^{\text{AF-IC}} \sim 430$ Oe. However, a well-defined first-order phase transition from the IC to FR phases, associated with the coexistence of both types of ordering, was not detected as shown in Fig. 2(c): with increasing external field, the broad IC peak at $k \sim 0.37$ shifts towards $k=\frac{1}{3}$ and continuously changes into the FR peak as the peak width sharpens. When the external field decreases from the saturated PM state, on the other hand, the first-order FR-IC phase transition was clearly observed. Nevertheless, even after decreasing external field down to zero field, the IC state with $q \sim 0.48$ survives and no AF ordering appears as shown in Fig. 3.

In contrast, when the external field increases at lower temperatures below $T=0.5$ K, the system enters directly the FR phase from the AF phase as shown in Figs. 2(d) and 3, although the critical field of the AF ordering dramatically increases. In contrast to the strongly broadened FR peak at $T=0.75$ K, is this peak below $T=0.5$ K observed immediately after the AF-FR phase transition close to instrumental resolution. With decreasing external field, the intensity of the FR peak gradually decreases and the background intensity increases. However, even in zero field the FR peak still remains, showing the anomalous hysteresis at lower temperatures. In order to investigate the intermediate state with one-third or two-thirds of the FR magnetization, found at $T=0.5$ K by Hanawa *et al.*,[5] we performed the (3 k 0)

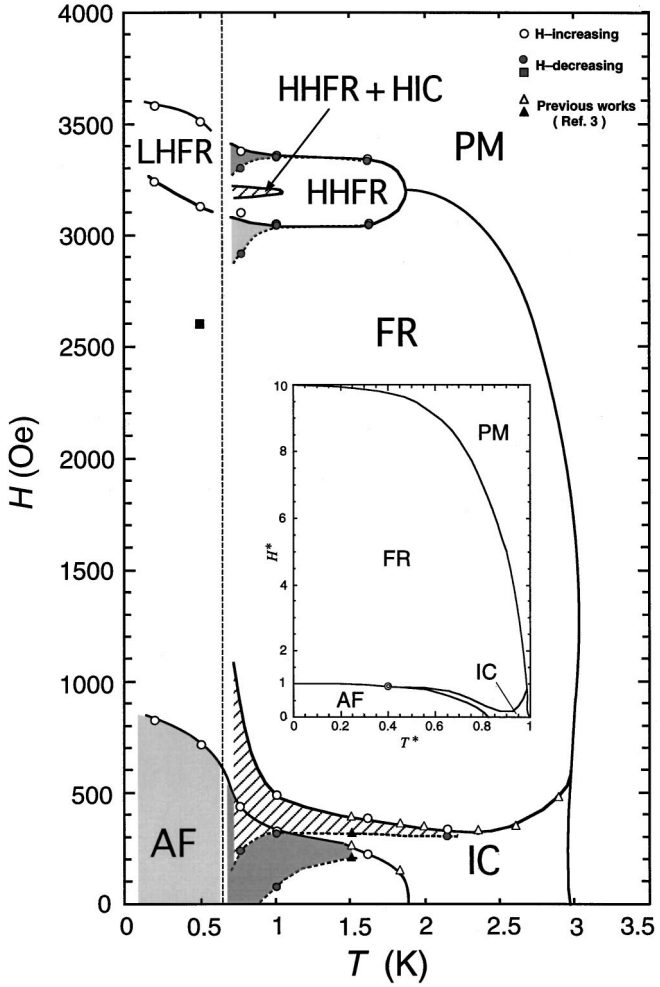

FIG. 3. (a) $H_{\|c}-T$ magnetic phase diagram of $CoNb_2O_6$. The open and closed symbols represent critical fields, determined on increasing and decreasing external fields, respectively. The light-, dark-shaded, and hatched areas at lower fields as well as the light- and dark-shaded areas at higher fields show the hysteresis, of the AF-FR, AF-IC, IC-FR, FR-HHFR, and HHFR-PM phase boundaries, respectively. Because of low temperatures, the critical field of the FR-PM phase transition is shown in the diagram (closed square). The hatched area at higher fields shows the coexistence of the HHFR and HIC phases. The inset shows the $H_{\|c}-T$ magnetic phase diagram obtained by previous mean-field calculations for the isosceles-triangular-lattice Ising model (Ref. 3), where the triple point is indicated by the double circle. The vertical and horizontal axes are scaled by the AF-FR transition field ($H_{\|c}=315$ Oe) and T_1, respectively.

reciprocal-lattice scans at $H_{\|c}=1500$ Oe during several runs between $H_{\|c}=0$ Oe and $H_{\|c}=1500$ Oe with a field-sweep rate of 67.0 Oe/sec, after ZFC down to $T=0.5$ K. Within our experimental accuracy, however, only the FR peak was observed and any other magnetic states with q different from $\frac{1}{3}$ of the FR state were not detected. Taking into account that magnetic Bragg intensity is proportional to the square of magnetic moments in the system, such an intermediate state would be a frozen domain state where both up-up-down FR ordering and down-down-up FR ordering with magnetization reversed against external field, coexist in the crystal. Since in the quasi-1D system $CoNb_2O_6$, the magnetic chains along the c axis with long-range intrachain correlations should be reversed during phase transition, it may be difficult to form the long-range up-up-down FR ordering at low temperatures in particular where thermal effect becomes ineffective. Therefore a sweep rate of external field as well as initial spin state will affect the volume fraction of up-up-down and down-down-up FR domains, thus magnetization observed. In fact, the observed intermediate state showed different absolute value of magnetization in different runs.[5]

In present measurements, large hysteresis at low temperatures strongly disturbs the accurate determination of the phase boundary in an equilibrium state. However, the different nature of the field-induced phase transitions at high temperatures (AF→IC→FR) and at low temperatures (AF→FR) indicates that the triple point where the AF, IC, and FR phases meet together, should be located at the temperature between 0.5 and 0.75 K in the $H_{\|c}-T$ magnetic phase diagram. Further, this feature qualitatively agrees with previous mean-field calculations[3] for the isosceles-triangular-lattice Ising model with J_0, J_1, and J_2 as is seen in the magnetic phase diagram shown in the inset of Fig. 3. Note that although the $H_{\|c}-T$ dependence of the broadening of the IC peak in the b^* direction approaching the triple point was not accurately determined because of anomalous hysteresis, the observation of the quite broad IC peak at low temperatures surely confirms the large ground-state degeneracy in the IC phase in the vicinity of the triple point.[3]

In this geometrically frustrated system $CoNb_2O_6$, the domain growth towards the equilibrium AF state proceeds extremely slowly as previous neutron-scattering measurements at $T=1.5$ K (Ref. 4) revealed. Therefore anomalous hysteresis at low temperatures implies that the relaxation towards the equilibrium AF state becomes slower with decreasing temperature. In order to investigate how the relaxation speed changes with temperature, we measured the time dependence of (3 k 0) reciprocal-lattice scan in zero field at several temperatures below T_2, after field quench from the FR state at $H_{\|c}=1500$ Oe. Figures 4 and 5(a) show the typical data of the time dependence of the (3 k 0) scan and integrated intensities, respectively. As shown in Figs. 4(a) and 5(a), after field quench below $T=0.5$ K, the FR state survives and the integrated intensity is weakly time dependent within our observation time of 1 h. On increasing temperature up to $T=0.6$ K, however, the FR peak abruptly starts to melt and instead the magnetic component develops around $k\sim0.48$ close to the AF peak position of $k=\frac{1}{2}$ as shown in Fig. 4(b). As the temperature slightly increases from 0.6 K, the time at which the integrated intensity of the IC peak exceeds that of the FR peak becomes dramatically shorter. At high temperatures above $T\sim0.65$ K, only the IC peak with time-dependent q which approaches $\frac{1}{2}$ of the AF ordering was detected after field quench as shown in Fig. 4(c). These observations indicate that the relaxation towards the equilibrium AF state becomes faster with increasing temperature. Particularly, the dramatic melting of the frozen FR state around $T\sim0.6$ K suggests that the relaxation time of the system becomes comparable with our observation time (several minutes) around $T\sim0.6$ K.

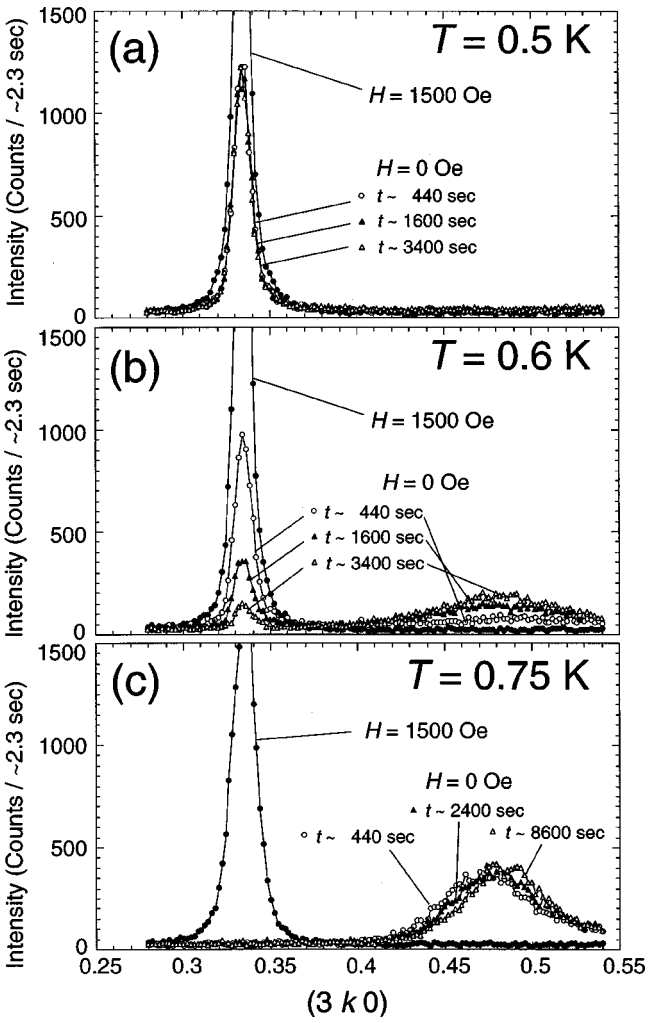

FIG. 4. Time dependence of the (3 k 0) reciprocal-lattice scans after field quench from $H_{\|c}=1500$ Oe, measured at (a) $T=0.5$ K, (b) $T=0.6$ K, and (c) $T=0.75$ K. The time t shown in the figures represents the time where the neutron intensity at the scan center was counted after the external field reached zero field at $t=0$.

As mentioned in the introduction, Hanawa *et al.* observed an additional low-temperature anomaly of specific heat in zero field at $T_s \sim 0.65$ K.[5] This temperature is very close to $T \sim 0.6$ K where the melting of the frozen FR state with time was detected in our experiments. To elucidate the origin of such an anomaly of specific heat, we measured the zero-field temperature variation of both (h $\frac{1}{2}$ 0) and (3 k 0) reciprocal-lattice scans on increasing temperature after ZFC down to the lowest temperature, which is the same cooling procedure as that by Hanawa *et al.*[9] As the temperature increases from $T=0.2$ K, the integrated intensity of the AF state gradually develops and finally saturates around $T \sim 0.6$ K. Within the temperature range observed ($T=0.2$–1.0 K), however, the mean AF domain size along both a and b axes on the isosceles triangular lattice is almost temperature independent as is seen in the temperature dependence of width parameters κ and W_b shown in Fig. 5(b): κ and W_b are half-width at half maximum of the magnetic Bragg scattering function along the a^* direction (Lorentzian shaped) and b^* direction

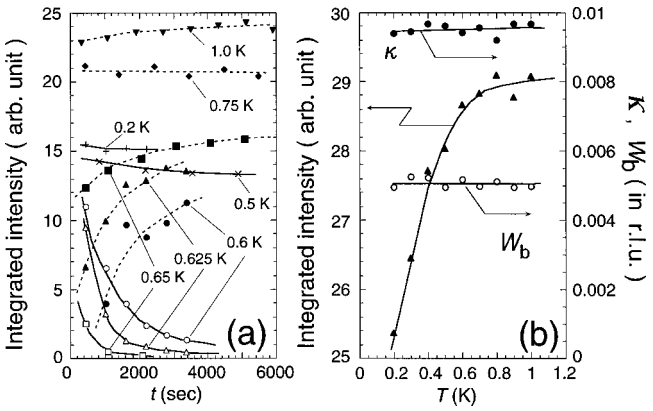

FIG. 5. (a) Time dependence of the integrated intensity of the FR and IC orderings after field quench at several temperatures below T_2. The solid lines (FR intensity) and dotted lines (IC intensity) are guide to eyes. (b) Temperature dependence of the (3 $\frac{1}{2}$ 0) integrated intensity and the width parameters (κ and W_b), measured with increasing temperature after ZFC down to $T=0.2$ K.

(Gaussian shaped), determined from the resolution-convoluted fittings.[3] Considering the extremely long relaxation time of this system at low temperatures, these results can be interpreted by the reversal of energetically unfavorable magnetic chains within each AF domain, frozen during a cooling process down to $T=0.2$ K. Such a reversal might be responsible for the low-temperature anomaly of specific heat at T_s. Note that although magnetic chains near the domain-wall boundary may also reverse with increasing temperature so as to develop mean domain size, a reversal of those chains is expected to take place less frequently than of magnetic chains inside domains because of a higher activation energy to reverse (Ref. 4).

B. High-field region

In Fig. 6, we show the (3 k 0) reciprocal-lattice scans at several temperatures below T_2 at fields of 2.6, 3.2, and 4.2 kOe. In Figs. 7(a) and (b), we also show the field dependence of integrated intensities at $T=1.62$ K and $T=0.5$ K, respectively, measured at (3 $\frac{1}{3}$ 0), (3 $\frac{2}{3}$ 0), (3 $\frac{1}{2}$ 0), (3 0 0), and (2 1 0) reciprocal-lattice points. As is clearly seen, with increasing external field at higher fields, both (3 $\frac{1}{3}$ 0) and (3 $\frac{2}{3}$ 0) integrated intensities of the FR ordering gradually decrease and the (2 1 0) integrated intensity develops and saturates around $H_{\|c} \sim 3.8$ kOe. This indicates the field-induced phase transition from the FR state to the saturated PM state in this high-field region. However, at all measured temperatures, the (3 0 0) integrated intensity appears and maximizes around the FR-PM transition. Particularly, at higher temperature of 1.62 K, the broad (3 $\frac{1}{2}$ 0) magnetic peak appears and coexists with the FR peaks as shown in Figs. 6(a) and 7(a). Taking into account that the (3 0 0) magnetic Bragg intensity is proportional to an imbalance of a magnetization along the c axis at Co^{2+} sites with two different easy axes, the high-temperature high-field ferrimagnetic (HHFR) state shown in Fig. 8(a) is considered to be field induced around the FR-PM phase transition at high temperatures. Such HHFR ordering

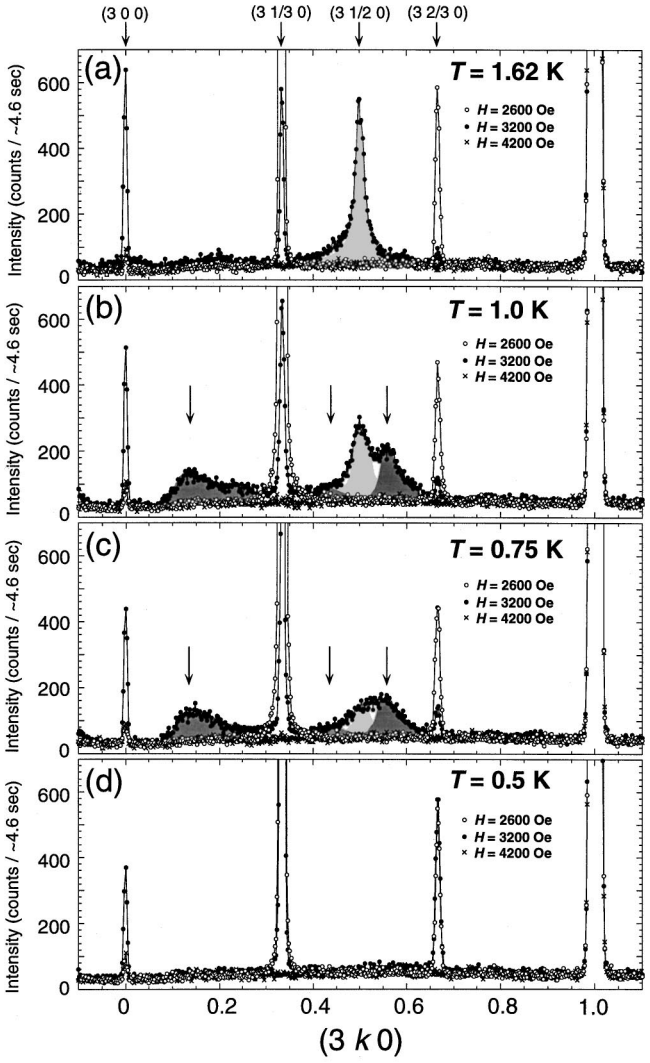

FIG. 6. Typical (3 k 0) reciprocal-lattice scans in high-field region, measured with increasing external field at (a) $T=1.62$ K, (b) $T=1.0$ K, (c) $T=0.75$ K, and (d) $T=0.5$ K. The light- and dark-shaded areas denote the HHFR and HIC peaks, respectively. The peak positions of the HIC peaks are indicated by the vertical arrows.

with $q=\frac{1}{2}$ was also observed in the neutron-diffraction measurements down to $T\sim 1.5$ K by Heid *et al.*[6]

When the temperature decreases from $T=1.62$ K, the HHFR peak at $k=\frac{1}{2}$ gradually decreases and the broad magnetic responses develop at the incommensurate peak positions as shown in Figs. 6(b) and (c). We found that they appear in very narrow field range around $H_{\|c}=3.2$ kOe and always coexist with both FR and HHFR peaks. The observed peaks at $k\sim 0.14$, $k\sim 0.44$, and $k\sim 0.56$ in the (3 k 0) scan [Figs. 6(b) and (c)] can be assigned to the (3 $1-2q$ 0), (3 q 0), and (3 $1-q$ 0) magnetic peaks with $q\sim 0.44$, respectively. These results show the appearance of a high-field incommensurate (HIC) state with a propagation vector $\mathbf{Q}_{\mathrm{propa}}=(0\ q\ 0)$ in this intermediate temperature region.

In contrast, at lower temperatures where the direct field-induced AF-FR phase transition takes place in low-field region, both HIC and HHFR peaks completely disappear and

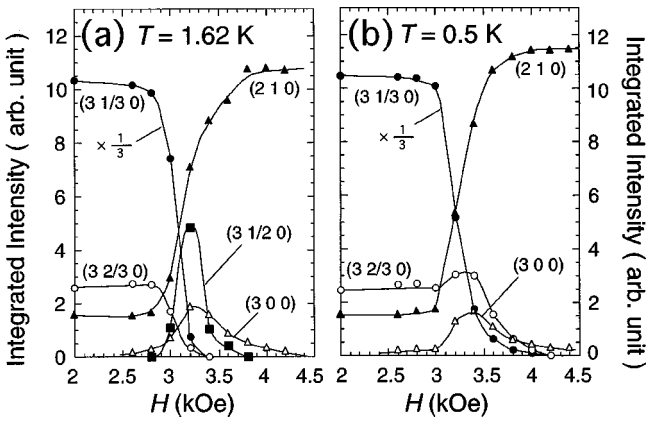

FIG. 7. Magnetic-field dependence of the integrated intensities of both (3 k 0) and (2 1 0) magnetic reflections in the high-field region at (a) $T=1.62$ K and (b) $T=0.5$ K, measured with increasing external field.

only the magnetic peaks at the FR peak position of $k=\frac{1}{3}$ and $k=\frac{2}{3}$ were observed as shown in Fig. 6(d). However, as shown in Fig. 7(b), the (3 $\frac{2}{3}$ 0) integrated intensity maximizes around $H_{\|c}=3.4$ kOe and persists up to rather higher field of $H_{\|c}=4$ kOe, although the (3 $\frac{1}{3}$ 0) one rapidly decreases as the FR-PM phase transition proceeds. The persistence of both (3 $\frac{2}{3}$ 0) and (3 0 0) integrated intensities even at higher fields indicates the appearance of the low-temperature high-field ferrimagnetic (LHFR) state with $q=\frac{1}{3}$ shown in Fig. 8(b) where one-sixth of magnetic chains in the magnetic unit cell direct downward against external field. However, the single domain state of the LHFR ordering hardly explains the observed intensity consistently. Therefore the low-temperature state in high-field region would be a domain state of the FR, LHFR, and saturated PM orderings.

In the high-field region, all the high-field magnetic phases (HHFR, HIC, and LHFR) coexist with the FR and saturated PM phases. The volume fraction of those high-field phases obtained is quite smaller than either that of the saturated PM phase or that of the FR phase at all the measured temperatures and external fields. Numerical values of the volume fraction at the typical field both at $T=1.62$ K and $T=0.5$ K are given in Table I. In addition, we found that the system exhibits strong hysteresis at low temperatures in particular as in the low-field region: with decreasing external field from the saturated PM state, no LHFR state appeared. We cannot rule out that extremely long relaxation time of the system is

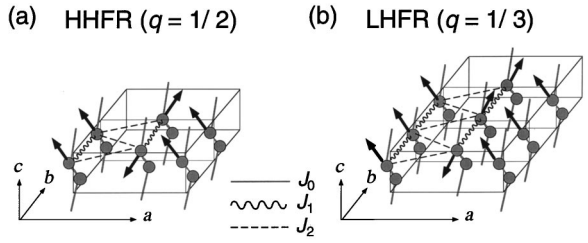

FIG. 8. Magnetic structures in (a) HHFR and (b) LHFR phases. The LHFR state yields magnetic reflection at the same peak position as that of the FR state.

TABLE I. Volume fraction of the FR, HHFR, LHFR, and saturated PM states. We assumed a domain state with an equal magnitude of magnetic moment of the FR, HHFR, and PM phases at $T=1.62$ K, and the FR, LHFR, and PM phases at $T=0.5$ K, respectively.

	FR (%)	HHFR (%)	LHFR (%)	Saturated PM (%)
$T=1.62$ K, $H_{\|c}=3.2$ kOe	6.0	24.0		70.0
$T=0.5$ K, $H_{\|c}=3.4$ kOe	2.0		30.0	68.0

the reason for a rather small volume fraction of the high-field states. Nevertheless, assuming the phase boundary as the field where the volume fraction of the high-field states becomes a half of the maximum, we obtain the magnetic phase diagram shown in Fig. 3.

Within the isosceles-triangular-lattice Ising model with J_0, J_1, and J_2, all the magnetic states at higher fields (FR, HHFR, HIC, LHFR, and saturated PM states) are degenerated at $T=0$ K at the FR-PM transition field and the high-field states (HHFR, HIC, and LHFR) are not stabilized as shown in the magnetic phase diagram in the inset in Fig. 3. Therefore small perturbation such as further neighbor exchange interactions and dipolar interactions[10] might partially lift the ground-state degeneracy and induce various high-field states in this geometrically frustrated system. Detailed study of the high-field states will appear elsewhere.

IV. CONCLUSION

We have studied low-temperature magnetic phase transitions of the geometrically frustrated isosceles triangular Ising antiferromagnet $CoNb_2O_6$ by means of neutron diffraction down to $T=0.2$ K under applied fields up to $H_{\|c}=4.4$ kOe. Anomalously large hysteresis as well as slow relaxation of the system was observed at low temperatures. Particularly, below $T\sim0.6$ K, the relaxation time of the system was found to become extremely long compared with our observation time, being responsible for the appearance of field-induced intermediate state with various magnetizations at $T=0.5$ K as well as for the additional low-temperature anomaly of specific heat at $T\sim0.65$ K, observed in the bulk measurements by Hanawa *et al.* In contrast to the two-step field-induced phase transitions from the AF to IC phases and from the IC to FR phases at higher temperatures below $T_2=1.9$ K, the system directly enters the field-induced FR phase from the AF phase at low temperatures. These observations indicate that the triple point where the AF, IC, and FR phases meet together should be located between $T=0.5$ K and $T=0.75$ K in the $H_{\|c}-T$ magnetic phase diagram of $CoNb_2O_6$, and qualitatively agree with previous mean-field studies for the isosceles-triangular-lattice Ising model with intrachain ferromagnetic interaction J_0 and interchain antiferromagnetic interactions J_1, J_2. Moreover, at higher fields, magnetic phases with various propagation vectors were found around the field-induced FR-PM phase transition, reflecting competing interactions in this geometrically frustrated system.

ACKNOWLEDGMENTS

We thank Professor Kay Kohn of Waseda University for supplying the single crystal used in the present studies. We also thank Dr. P. Smeibidl for technical support for low-temperature experiments at Hahn-Meitner-Institute. This work was partly supported by the Science Research Promotion Fund of the Promotion and Mutual Aid Corporation for Private Schools of Japan.

*Present address: Satellite Venture Business Laboratory, Gunma University, 1-5-1, Tenjin-cho, Kiryu, Gunma 376-8515, Japan.

[1] M. F. Collins and O. A. Petrenko, Can. J. Phys. **75**, 605 (1997).
[2] S. Mitsuda, S. Kobayashi, K. Aga, H. Katagiri, H. Yoshizawa, M. Ishikawa, K. Miyatani, and K. Kohn, J. Phys. Soc. Jpn. **64**, 2325 (1995).
[3] S. Kobayashi, S. Mitsuda, M. Ishikawa, K. Miyatani, and K. Kohn, Phys. Rev. B **60**, 3331 (1999).
[4] S. Kobayashi, S. Mitsuda, T. Jogetsu, J. Miyamoto, H. Katagiri, and K. Kohn, Phys. Rev. B **60**, R9908 (1999).
[5] T. Hanawa, K. Shinkawa, M. Ishikawa, K. Miyatani, K. Saito, and K. Kohn, J. Phys. Soc. Jpn. **63**, 2706 (1994).
[6] C. Heid, H. Weitzel, P. Burlet, M. Bonnet, W. Gonschorek, T. Vogt, J. Norwig, and H. Fuess, J. Magn. Magn. Mater. **151**, 123 (1995).
[7] K. Katsumata, J. Phys. Soc. Jpn. **39**, 42 (1975).
[8] B. M. Wanklyn, B. J. Garrard, and G. Garton, Mater. Res. Bull. **11**, 1497 (1976).
[9] M. Ishikawa (private communication).
[10] Heid *et al.* calculated the zero-Kelvin thermal energy including dipolar term and explained the appearance of the HHFR state at $T=0$ K in the high-field region in Ref. 6. However, our preliminary calculations with dipole interactions indicate that the LHFR state has lower zero-Kelvin thermal energy than that of the HHFR state at high fields.